

## Conductance crossovers in coherent surface transport on Y nanojunctions

To cite this article: Andrea Bertoni *et al* 2009 *J. Phys.: Conf. Ser.* **193** 012019

View the [article online](#) for updates and enhancements.

### Related content

- [Calculation of the current response in a nanojunction for an arbitrary time-dependent bias: application to the molecular wire](#)  
Michael Ridley, Angus MacKinnon and Lev Kantorovich
- [Spin electronic manipulation based on zigzag-edge graphene nanojunction with a line defect](#)  
Haidong Li, Lili Zheng and Ruixue Li
- [Study of the high-frequency performance of III-As nanojunctions using a three-dimensional ensemble Monte Carlo model](#)  
Toufik Sadi and Jean-Luc Thobel

# Conductance crossovers in coherent surface transport on Y nanojunctions

Andrea Bertoni<sup>1</sup>, Giampaolo Cuoghi<sup>1,2</sup>, Giulio Ferrari<sup>3</sup> and Guido Goldoni<sup>1,2</sup>

<sup>1</sup> S3 National Research Center, INFN-CNR, 41125 Modena, Italy

<sup>2</sup> Dipartimento di Fisica, Università di Modena e Reggio Emilia, Modena, Italy

<sup>3</sup> CNISM Unità di Ricerca di Modena, Modena, Italy

E-mail: andrea.bertoni@unimore.it

**Abstract.** Conductance characteristics of a nonplanar two-dimensional electron gas (2DEG) can expose the role of its bending on the 2DEG electronic states. In particular, the presence of an effective geometric potential can be revealed. Here, we present a numerical study of the coherent electron transport on Y nanojunctions of three cylindrical 2DEGs, including a proposal for the experimental detection of the geometric potential. We describe the analytical approach leading to the reduction of the problem dimensionality from 3D to 2D and sketch our simulation scheme.

## 1. Introduction

The quantum dynamics of a particle constrained on a thin semiconductor layer can be effectively represented by a two-dimensional (2D) equation of motion, as far as the layer thickness is so small that the dynamics in the directions parallel to the layer can be decoupled from the orthogonal one, where only the ground state of the confinement potential is occupied. While for planar layers, a trivial 2D version of the effective-mass Schrödinger equation can be sufficient to get the main electronic-states features, a 2D system that is curved within the 3D space, requires a different model. In fact, the system curvature must be included into the 2D dynamics through an effective geometric potential (GP) that attracts a carrier towards the regions with stronger curvature. Furthermore, the equation of motion should be modified in order to account for the transformation between the 2D and 3D coordinate system, as we will illustrate in the next section.

Before proceeding, we stress that the topic introduced above has a relevance that goes beyond theoretical physics. In fact, a number of nanostructures have been recently realized where carriers are confined on a surface wrapped around a core semiconductor nanowire via epitaxial overgrown[1], and the controlled growth of branched nanowires has been clearly demonstrated[2]. The fabrication of Y junctions of cylindrical 2DEGs is possibly the next step of these experimental activities. We will show in Section 3 that transport characteristics of the latter Y junctions are able in principle to expose the presence of the GP. Indeed, although the GP has been conjectured long time ago[3] and it is commonly included in the modeling of curved 2D systems[4], its direct experimental evidence has not been achieved so far.

Finally, in Section 4 we briefly analyze the dependence of the junction coherent transmission on the angle between two of the branches.

## 2. Equation of motion on a curved surface

Let us consider a curved surface whose parametric equation is  $\mathbf{r} = [x(q_1, q_2), y(q_1, q_2), z(q_1, q_2)]$  and a quantum particle in the 3D space. Following the limiting procedure proposed in Refs. [5] and [6], we take a confining potential that is zero in close proximity of the surface and infinite elsewhere. The particle dynamics is separable in the directions orthogonal and parallel to the surface. In particular, the former direction can be neglected, while in the latter direction, the steady-states of the quantum particle can be obtained through the following modified Schrödinger equation[7]

$$-\frac{\hbar^2}{2m} \sum_{i,j=1}^2 \frac{1}{\sqrt{g}} \frac{\partial}{\partial q_i} \left[ \sqrt{g} (\mathbf{g}^{-1})_{ij} \frac{\partial}{\partial q_j} \right] \psi - \frac{\hbar^2}{2m} [M^2 - K] \psi + V\psi = E\psi(q_1, q_2), \quad (1)$$

where  $\mathbf{g}(q_1, q_2)$  is the metric tensor on the surface,  $g(q_1, q_2)$  its determinant,  $M(q_1, q_2)$  and  $K(q_1, q_2)$  its local mean and Gaussian curvature, respectively, and  $V(q_1, q_2)$  a possible external potential. It is straightforward to note that the term containing the two curvatures acts as an additional potential term. Furthermore, since  $M^2 \geq K$ , this potential is always attractive. We note here that an external magnetic field can be also included in the above equation[8], with its effect being separable from that of the surface curvature[9].

We are interested in the scattering states of the 2D structure. To be specific, we consider a Y junction of three cylinders, as depicted in Fig. 1. The system has three open boundaries, namely the three circumferences  $A$ ,  $B$  and  $C$  at the edges of the three branches, with radii  $R_A$ ,  $R_B$  and  $R_C$ , respectively. We take the surface coordinate  $q_1$  along the circumferences and  $q_2$  orthogonal

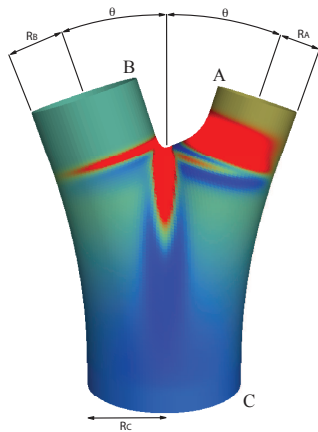


**Figure 1.** Curved surface forming a Y junction, where the two uppermost branches form an angle  $\theta$  with the lower cylinder. In the simulation presented we take  $R_A = 15$  nm  $R_B = 20$  nm  $R_C = 30$  nm. The negative value of the GP term  $-\frac{\hbar^2}{2m} [M^2 - K]$  is reported, in colorcode (red= $-30$  meV, blue= $0$ ) on the surface.

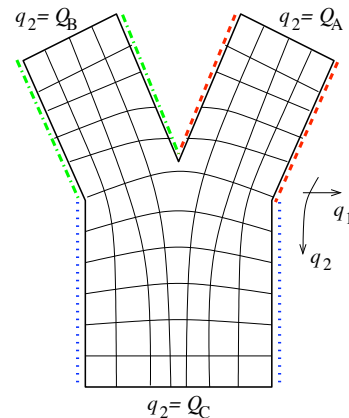


**Figure 2.** Sketch of the simulation domain with the 2D coordinate system  $[q_1, q_2]$ . The lateral edges with the same dashed/dotted line are to be considered mutually connected to form periodic conditions.

to them, as shown in Fig. 2, where the  $[q_1, q_2]$  simulation domain is sketched, together with its coordinate system. The boundary  $\alpha = A, B, C$  has coordinates  $(q_1 \in [0, 2\pi R_\alpha], q_2 = Q_\alpha)$ . On the cylindrical lead connected to  $A$  (not shown in Fig. 1) the wave function  $\psi$  for a given energy  $E$  can be written as [10]

$$\psi(q_1, q_2 < Q_A) = \sum_{m=0}^{M^A} a_m^A \chi_m^A(q_1) e^{ik_m^A q_2} + \sum_{m=0}^{M^A} b_m^A \chi_m^A(q_1) e^{-ik_m^A q_2} + \sum_{m=M^A+1}^{\infty} b_m^A \chi_m^A(q_1) e^{k_m^A q_2}, \quad (2)$$

and it has a similar expression in the other leads, non reported for brevity. The physical meaning of Eq. (2) is simple. The first term represents the incoming component as a combination of the different orthogonal modes of the lead  $\chi_m^A(q_1)$ , weighted with the injection coefficients  $a_m^A$ . The second term represents the combination of the outgoing traveling component, weighted with the outgoing coefficients  $b_m^A$  (they are the reflection coefficients in case no injection occurs from the other leads). The third term represents the evanescent waves. If we define  $\epsilon_m^\alpha$  as the energy of the transverse mode  $\chi_m^\alpha$ ,  $m = M^\alpha$  represents the last mode with  $\epsilon_m^\alpha < E$  and the evanescent waves have  $\epsilon_m^\alpha > E$ . On the other hand, for the traveling waves,  $\frac{(\hbar k_m^\alpha)^2}{2m} = (E - \epsilon_m^\alpha)$  is the kinetic part of the particle energy.

In order to obtain the scattering states of the structure, once we fix an energy  $E$ , we solve numerically Eq. (1) on the internal points of the domain (Fig. 2), together with Eq. (2) on the boundaries. We stress that the outgoing coefficients  $b_m^\alpha$  are unknowns of the problem. The solution of the two coupled equations is essentially the *quantum transmitting boundary method*[10].

In our simulations, we obtain the transmission coefficients by injecting the carriers only in the ground mode of lead  $A$ , i.e.  $a_0^A \neq 0$  and zero otherwise. On the other hand, for the conductance calculation we populate the incoming modes with a Fermi distribution following the Landauer-Büttiker approach.

### 3. Effect of the GP on the conductance

Here we show how the presence of the GP term  $\frac{\hbar^2}{2m} [M^2 - K]$  in Eq. (1) produces a remarkable effect on the conductance of a GaAs-based Y junction. In Fig. 3 we report the conductance between leads  $A$  and  $C$  (solid line) and between leads  $A$  and  $B$  (dashed line), calculated through a Landauer-Büttiker model at 2 K. Leads  $B$  and  $C$  are always kept at the same potential. We take a Fermi energy of 0.6 meV from the bottom of the conduction band and do not consider charging effects inside the device. Left (right) panel shows the results with (without) the GP term included in Eq. (1).

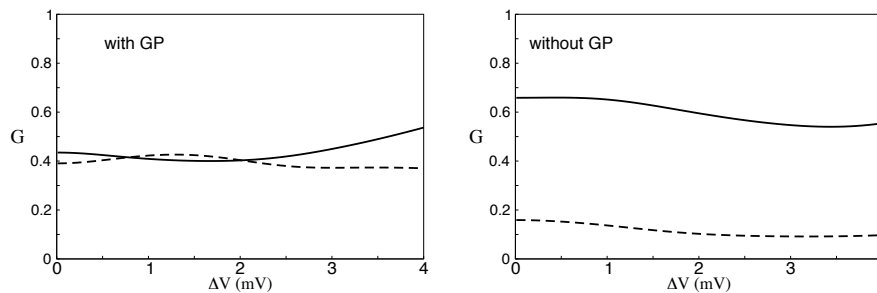


**Figure 3.** Conductance at a temperature of 2 K between two couples of cylindrical leads of the Y junction shown in Fig. 1. The solid (dashed) line represents the conductance between  $A$  and  $C$  ( $A$  and  $B$ ). The inclusion of the GP leads to crossovers of the two curves.

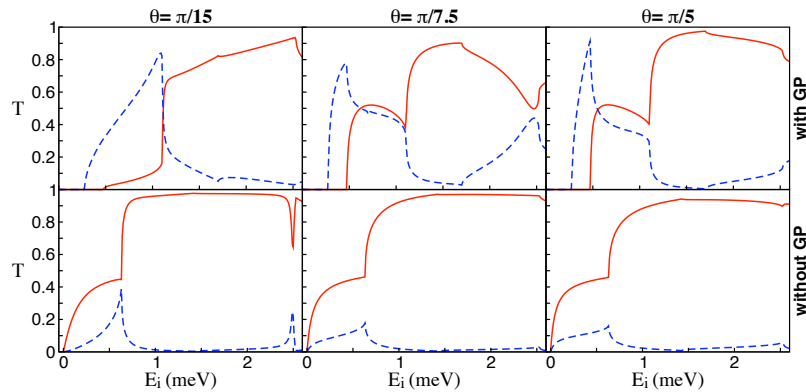


**Figure 4.** Transmission probability as a function of the injection energy with (a) and without (b) the GP at three different angles  $\theta$  (see Fig. 1). The carriers enter the Y junction from the ground transverse mode of  $A$  and are transmitted in  $B$  (dashed line) and  $C$  (solid line). The thresholds of the transverse modes in  $B$  and  $C$  emerge as peaks or discontinuities in the curves.

A double crossing between the two curves occurs if the GP is included, while they remain well separated otherwise. The reason of this behavior can be ascribed to the different surface curvatures in the cylindrical leads, that produce, through the GP term, different energy shifts on the fundamental transverse modes  $\chi_0^\alpha$ , as detailed in Ref. [11]. On the other hand, if the GP is not included, the ground-state energies  $\epsilon_0^\alpha$  are independent on the radii  $R_\alpha$ , since the 1D lines of the boundaries have periodic boundary conditions.

#### 4. Dependence of the coherent transmission on the branches angle

In order to understand the robustness of the effect described above, we calculated the transmission coefficient for different values of the angle  $\theta$  between the two uppermost branches and the lowermost one (see Fig. 1). When a very small angle ( $\theta \approx \pi/15$ , left panels of Fig. 4) is considered, the coherent transmission in  $B$  is in general reduced with respect to larger  $\theta$ . However, for angles comparable to experimental Y-branched nanowires ( $\pi/10 < \theta < \pi/4$ ) we find that the transmission spectrum is essentially unchanged, as can be gathered from the central and right panels of Fig. 4. A similar behavior can be expected for the conductance, this confirming the robustness of the presence of the conductance crossings as a signature of the GP.

#### References

- We are pleased to thank Fiorenzo Bastianelli and Massimo Rudan for helpful discussions and suggestions.
- [1] Fontcuberta i Morral A, Spirkoska D, Arbiol J, Heigoldt M, Morante J R and Abstreiter G 2008 *Small* **4** 899
  - [2] Wang D, Qian F, Yang C, Zhong Z and Lieber C M 2004 *Nano Letters* **4** 871
  - [3] DeWitt B S 1957 *Rev. Mod. Phys.* **29** 377
  - [4] see e.g. Duclos P and Exner P 1995 *Rev. Math. Phys.* **7** 73  
Aoki H, Koshino M, Takeda D, Morise H and Kuroki K 2001 *Phys. Rev. B* **65** 35102  
Meyer G J, Dias N L, Blick R H and Knezevic I 2007 *IEEE Trans. on Nanotech.* **6** 446  
Ferrari G, Goldoni G, Bertoni A, Cuoghi G and Molinari E 2009 *Nano Lett.* **9** 1631
  - [5] Jensen H and Koppe H 1971 *Ann. Phys.* **63** 586
  - [6] da Costa R C T 1981 *Phys. Rev. A* **23** 1982
  - [7] Marchi A, Reggiani S, Rudan M and Bertoni A 2005 *Phys. Rev. B* **72** 035403
  - [8] Ferrari G, Bertoni A, Goldoni G and Molinari E 2008 *Phys. Rev. B* **78** 115326
  - [9] Ferrari G and Cuoghi G 2008 *Phys. Rev. Lett.* **100** 230403
  - [10] Lent C S and Kirkner D J 1990 *J. Appl. Phys.* **67** 6353
  - [11] Cuoghi G, Ferrari G and Bertoni A 2009 *Phys. Rev. B* **79** 073410